Modeling Explosive Opinion Depolarization in Interdependent Topics

Jaume Ojer,[1] Michele Starnini,[1,2,*] and Romualdo Pastor-Satorras[1,†]
[1]Departament de Física, Universitat Politècnica de Catalunya, Campus Nord B4, 08034 Barcelona, Spain
[2]CENTAI Institute, 10138 Turin, Italy

(Received 14 December 2022; accepted 22 March 2023; published 17 May 2023)

Understanding the dynamics of opinion depolarization is pivotal to reducing the political divide in our society. We propose an opinion dynamics model, which we name the social compass model, for interdependent topics represented in a polar space, where zealots holding extreme opinions are less prone to change their minds. We analytically show that the phase transition from polarization to consensus, as a function of increasing social influence, is explosive if topics are not correlated. We validate our theoretical framework through extensive numerical simulations and recover explosive depolarization also by using initial opinions from the American National Election Studies, including polarized and interdependent topics.

DOI: 10.1103/PhysRevLett.130.207401

The presence of opinion polarization—i.e., two groups holding opposite and possibly extreme opinions in a population—has been extensively observed with respect to several controversial topics, ranging from religion [1] and race [2] to climate change [3] and political ideology [4]. Polarization may contribute to deepening the political divide in our society [5], hampering the collective resolution of important societal challenges [6], and even fostering the spreading of misinformation and conspiracy theories [7]. Consequently, an interest toward a theoretical understanding of the emergence of opinion polarization has arisen in several disciplines, from statistical physics to social and computer science.

Models that reproduce polarization are based on different opinion dynamics mechanisms, such as homophily [8,9], bounded confidence [10–12], or opinion rejection [13,14]. Modeling the process of reducing opinion polarization among the population, or *depolarization* [15], has also been the object of recent work [16–18]. In most cases, such modeling efforts address the simplest case of one-dimensional opinions with respect to a single topic [19,20]. However, the process of opinion formation may invest multiple topics at the same time [21,22], requiring a proper multidimensional modeling framework for opinion dynamics [23–26]. When multiple topics are taken into account, a crucial feature can often be observed: issue alignment [27,28], i.e., the presence of correlations between opinions with respect to different topics, especially along the so-called left-right dimension [29,30]. For instance, individuals with strong religious beliefs are more likely to oppose abortion legalization [31], while other nontrivial correlations can emerge [22,28,32]. However, many multidimensional opinion models proposed so far failed to reproduce opinion polarization [33–35], neglecting the interdependence among different topics [36,37].

In this Letter, we aim to fill this gap by proposing an analytically tractable model of opinion dynamics in a space of two interdependent topics. We represent this space in the polar plane, where the angle represents the orientation of an individual with respect to both topics, and the radius expresses the attitude strength (referred to as conviction in the literature [38]). This polar representation allows us naturally to formulate the key assumption of the model: i.e., zealots with extreme opinions (large conviction) may be less prone to change their opinion than individuals with small conviction, in line with experimental psychology [39,40]. We observe that this model, which we name the *social compass model*, exhibits a phase transition from an initial polarized state to a depolarized or consensus one, as a function of increasing social influence. We analytically show, at the mean-field level, that the nature of such transition depends on the correlation between initial opinions: uncorrelated opinions trigger a first-order, or explosive, depolarization to consensus, while correlated initial opinions lead to a second-order, continuous transition. We test our theoretical framework by using real data of polarized initial opinions with respect to interdependent topics.

We start by defining a representation of opinions in polar space. Let us consider N individuals, each agent i holding opinions (x_i, y_i) toward two distinct topics X and Y, respectively, that are assumed to be normalized in the interval $x_i, y_i \in [-1, 1]$. The combined opinion of each individual with respect to the two topics can be represented in polar coordinates by its conviction $\rho_i = \sqrt{x_i^2 + y_i^2}$ and its orientation $\varphi_i = \arctan(y_i/x_i)$, with $\varphi_i \in [-\pi, \pi]$. For instance, two agents i and j holding extreme and opposite opinions, $x_i = y_i = 1$, $x_j = y_j = -1$, will be represented in the polar plane with the same, maximum conviction $\rho_i = \rho_j = \sqrt{2}$ and opposite orientations $\varphi_i = \pi/4$ and $\varphi_j = -3\pi/4$. Note that representing individuals in a plane defined by two major axes, such as libertarian versus

authoritarian within a social context, and left versus right within an economic context, is not novel in political science [41].

To support this polar representation, we consider empirical opinions from the American National Election Studies (ANES) [42]; see Supplemental Material, Sec. I (SM I) [43]. The angular distribution $P(\varphi)$ obtained from the ANES dataset for different pairs of topics shows a rich phenomenology. We highlight four interesting cases, reported in Fig. SF 1 of Supplemental Material SM IA [43]. First, there can be no consensus with respect to either topic, with opinions roughly uniformly distributed, so that $P(\varphi)$ will also be a uniform distribution; see Fig. SF 1(a). Second, a consensus around both topics may emerge, indicated by the $P(\varphi)$ distribution peaked around a certain consensus value $\varphi^* = \arctan(y^*/x^*)$, where y^* and x^* are the consensus opinions of topics Y and X, respectively; see Fig. SF 1(b). Third, opinions with respect to both topics can be polarized; i.e., both one-dimensional opinion distributions are characterized by two well-separated peaks. Here we can distinguish two different cases: opinions can be polarized but not correlated, for which the $P(\varphi)$ distribution will be characterized by four peaks (quadrimodal distribution), representing, for example, the four extreme combinations $(x_i, y_i) = (+1,+1), (+1,-1), (-1,+1), (-1,-1)$; see Fig. SF 1(c). Finally, opinions can be polarized *and* strongly correlated, shown in Fig. SF 1(d). In this case, one can observe only two peaks in the $P(\varphi)$ (bimodal distribution), corresponding to two ideological combinations like $(x_i, y_i) = (+1,+1), (-1,-1)$.

Within this context, we study how social influence can affect the initial opinions of individuals, by proposing the social compass model, which is inspired by the Friedkin-Johnsen model [44]. For each individual i, we focus on the time evolution of their orientation, represented by $\theta_i(t)$, provided their initial orientation $\theta_i(0) = \varphi_i$ and that their conviction ρ_i will not change over time. We rely on only two key assumptions: (i) agents exert a certain degree of social influence on their peers and (ii) each agent i has a tendency to maintain their initial opinion φ_i proportional to their conviction ρ_i (i.e., agents with high conviction are more stubborn). We operationalize this simple theoretical framework in the following set of N ordinary differential equations,

$$\dot{\theta}_i(t) = \rho_i \sin[\varphi_i - \theta_i(t)] + \frac{\lambda}{N}\sum_{j=1}^{N} \sin[\theta_j(t) - \theta_i(t)], \quad (1)$$

where λ is a coupling constant that quantifies the strength of social influence. In a real-world scenario, social influence, indicating the tendency of individuals to adjust their behavior to meet the expectations of their peers, could be empirically quantified by surveys. We assume that each individual can interact with all other individuals, which allows us to solve the model through a mean-field approach. Since opinions are described by angles, it is natural to model consensus formation as the alignment of the agents' orientations [11,45,46], with a phase coupling inspired in the Kuramoto model [47].

The social compass model exhibits a phase transition at a threshold value λ_c of the coupling constant, separating a polarized from a depolarized (consensus) phase. This transition can be characterized in terms of the order parameter r, defined by [48]

$$r(\lambda)e^{i\psi(\lambda)} = \frac{1}{N}\sum_{j=1}^{N} e^{i\theta_j(\lambda)}, \quad (2)$$

where $\theta_j(\lambda)$ is computed at the steady state of Eq. (1) and $\psi(\lambda)$ is the average orientation in the population. In the absence of social interactions ($\lambda = 0$), Eq. (1) leads to the steady state $\theta_j = \varphi_j$. In accordance with the empirical evidence presented above, we are interested in initial states with polarized orientations following bimodal or quadrimodal $P(\varphi)$ distributions. For this polarized state, we have $r(\lambda = 0) = 0$ provided that $\langle\cos(\varphi)\rangle = \langle\sin(\varphi)\rangle = 0$, where $\langle\cdots\rangle$ denotes the average value. For sufficiently large λ, a consensus state leads to $r \simeq 1$, meaning that all the agents have the same average orientation $\theta_j \simeq \psi$.

Given that the initial opinions are distributed according to uncorrelated probability densities $P(\rho)$ and $P(\varphi)$, a general solution of the model can be found by the self-consistent equation $r = I(r,\psi)$ (see Supplemental Material SM II [43]) [48], with

$$I(r,\psi) = \int_0^\infty d\rho \int_{-\pi}^{\pi} d\varphi \frac{P(\rho)P(\varphi)[\lambda r + \rho e^{i(\varphi-\psi)}]}{\sqrt{(\lambda r)^2 + 2\lambda r\rho\cos(\varphi-\psi) + \rho^2}}, \quad (3)$$

which translates into the pair of equations $r = \mathrm{Re}\{I(r,\psi)\}$ and $0 = \mathrm{Im}\{I(r,\psi)\}$ for the real and imaginary parts of $I(r,\psi)$, respectively. The equation for the imaginary part is used to identify the average orientation ψ, which, plugged into the equation for the real part, allows us to compute the order parameter r as a function of λ. We can establish a threshold condition for the depolarized state considering the instability of the solution $r = 0$, which translates into the condition $\partial\mathrm{Re}\{I(r,\psi)\}/\partial r|_{r=0} \geq 1$. This leads to a depolarized state for $\lambda > \lambda_c$ with (see SM IIA)

$$\lambda_c = \frac{1}{\int_0^\infty d\rho \frac{P(\rho)}{\rho}\int_{-\pi}^{\pi} d\varphi P(\varphi)\sin^2(\varphi-\psi)}. \quad (4)$$

We tested the validity of this theoretical result by using empirical data from the ANES opinion polls as values of the initial orientation and conviction, $P(\varphi)$ and $P(\rho)$, respectively. We focused in particular on correlated polarized opinions represented by bimodal $P(\varphi)$, reported in

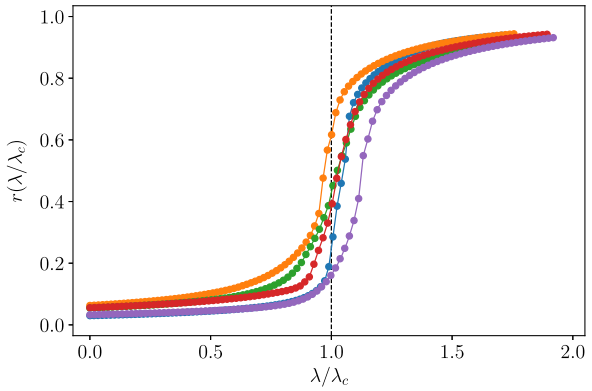

FIG. 1. Order parameter $r(\lambda/\lambda_c)$, by using different initial opinion distributions from ANES data (topics described in Supplemental Material, Fig. SF 3 [43]). The theoretical threshold λ_c is computed numerically from Eq. (4), by using the empirical distributions $P(\rho)$ and $P(\varphi)$; see Supplemental Material SM IIB.

Fig. SF 3 [43]. As we can see in Fig. 1, in all cases we observe numerically a depolarization transition at a threshold that is approximately described by the theoretical prediction Eq. (4).

To address analytically the nature of the observed depolarization transition, we consider specific forms of the conviction and orientation distributions. From the ANES dataset, the conviction distribution shows in general an increasing trend; see SM IB. We thus model it as a power-law form,

$$P(\rho) = (\alpha + 1)\rho^{\alpha}, \tag{5}$$

where $\alpha = 0$ corresponds to a uniform distribution, and the limit $\alpha \to \infty$ represents the case constant conviction, $P(\rho) = \delta(\rho - \rho_{\max})$. We arbitrarily fix $\rho_{\max} = 1$. Regarding the orientation distribution, we choose the general form,

$$P(\varphi) = \frac{1}{4}[\delta(\varphi - \varphi_0) + \delta(\varphi - \varphi_0 + \pi)] + \frac{1}{4}[\delta(\varphi + \varphi_0) + \delta(\varphi + \varphi_0 - \pi)], \tag{6}$$

fulfilling the initial polarized state condition $\langle\cos(\varphi)\rangle = \langle\sin(\varphi)\rangle = 0$. For symmetry reasons, we restrict $\varphi_0 \in [0, \pi/4]$ and consider separately the cases of correlated (bimodal distribution, $\varphi_0 = 0$) and uncorrelated (quadrimodal distribution, $\varphi_0 > 0$) polarization. The analysis of the equation $0 = \mathrm{Im}\{I(r, \psi)\}$ leads in both cases to an average orientation $\psi = \pm\pi/2$ independent of λ (see Supplemental Material, Secs. SM III and SM IV [43]), which we will impose in the following analysis. We note that the average orientation ψ in the depolarized phase falls exactly at the middle point between the two peaks. Therefore, the consensus emerges as a positive solution where no initial opinion dominates over the other.

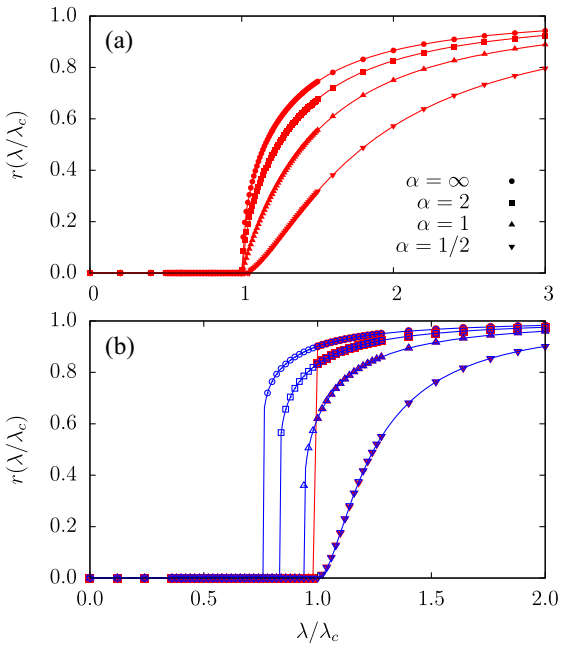

FIG. 2. Order parameter $r(\lambda/\lambda_c)$ for different values of α. The initial orientation distribution $P(\varphi)$ is polarized and correlated [(a) $\varphi_0 = 0$] or fully uncorrelated [(b) $\varphi_0 = \pi/4$]. Points (solid lines) represent numerical simulations (theoretical predictions). System size $N = 10^6$. For the uncorrelated case, backward continuation (blue) is plotted in empty symbols. Curves of forward continuation (red) for different α collapse for $\lambda \le \lambda_c$, while they are identical to backward continuations for $\lambda > \lambda_c$.

In the case of correlated and polarized initial opinions, corresponding to a bimodal $P(\varphi)$, the function $\mathrm{Re}\{I(r, \psi)\}$ can be integrated analytically, yielding the self-consistent equation,

$$r = {}_2F_1\left(\frac{1}{2}, \frac{\alpha+1}{2}; \frac{\alpha+3}{2}; -\frac{1}{(\lambda r)^2}\right), \tag{7}$$

where ${}_2F_1(a, b; c; z)$ is the Gaussian hypergeometric function [49]. To study the behavior in the vicinity of the depolarization transition, we perform a leading order expansion of the hypergeometric function around $r = 0$ and solve the ensuing equation (see SM IIIA). We obtain that the transition is continuous, with the typical behavior of the order parameter $r(\lambda) \sim (\lambda - \lambda_c)^{\beta}$, with a threshold and an exponent β depending on α as

$$\lambda_c(\alpha) = \frac{\alpha}{\alpha + 1}, \qquad \beta(\alpha) = \begin{cases} 1/\alpha & \text{if } \alpha < 2 \\ 1/2 & \text{if } \alpha > 2. \end{cases} \tag{8}$$

The particular values $\alpha = 1$ and $\alpha \to \infty$ can be solved analytically, recovering the asymptotic result of Eq. (8) (see SM IIIA1). Figure 2(a) shows numerical simulations of r compared with the theoretical prediction from the numerical or analytical solution of Eq. (7). The match obtained is perfect, confirming a continuous transition in this case. We

TABLE I. Numerical exponent β for a system size $N = 10^6$ and different values of α, estimated from a linear regression of a double logarithmic plot of r as a function of $\lambda - \lambda_c$ in the vicinity of the threshold. Numerical estimation is in good agreement with the theoretical prediction given by Eq. (8). Deviations from it (as for $\alpha = 1/3$) could be ascribed to finite size effects.

α	1/3	1/2	1	2	3	∞
β	2.74(1)	1.96(1)	0.99(1)	0.57(1)	0.51(1)	0.50(1)

estimated the values of the exponent β by performing a linear regression of r as a function of $\lambda - \lambda_c$ in the vicinity of the transition. The values obtained, reported in Table I, confirm the validity of our theoretical approach.

For polarized, but not correlated, initial opinions, $P(\varphi)$ corresponds to a quadrimodal distribution given by Eq. (6) with $\varphi_0 > 0$. The resulting integral of $\mathrm{Re}\{I(r,\psi)\}$ does not allow an analytical treatment, so we resort to solving numerically the corresponding self-consistent equation; see SM IVA [43]. Figure 2(b) shows numerical simulations of r (symbols) compared with the corresponding numerical solution (lines) of the self-consistent equation for the quadrimodal symmetric case with $\varphi_0 = \pi/4$. For small values of α, we observe a continuous transition, as in the bimodal case. However, for sufficiently large α, the transition becomes discontinuous; i.e., we observe an explosive depolarization. The first-order nature of the transition is reflected in the presence of hysteresis observed when performing forward and backward continuation experiments; see SM V.

We further explore the nature of this discontinuous transition by focusing on the case in which all agents hold maximum conviction ($\alpha = \infty$). From Eq. (4), we can compute analytically the transition threshold λ_c depending on the symmetry of the initial orientation distribution $P(\varphi)$, namely the angle φ_0:

$$\lambda_c(\varphi_0) = \frac{1}{\cos^2(\varphi_0)}. \tag{9}$$

The nature of the transition can be uncovered by performing a Taylor expansion on the right-hand side of the self-consistent equation $r = \mathrm{Re}\{I(r,\psi)\}$ for r small in the vicinity of $\lambda_c(\varphi_0)$, and solving for the analytic continuation of the solution $r = 0$. A nonzero solution for $\lambda > \lambda_c$ is indicative of a continuous transition, while the solution for $\lambda < \lambda_c$ corresponds to the unstable branch of a discontinuous transition. This analysis shows the presence of a threshold angle $\varphi_c = \arcsin(1/\sqrt{5})$, such that for $\varphi_0 < \varphi_c$ the transition is continuous, whereas it is explosive for $\varphi_0 > \varphi_c$ (see SM IVB for details [43]).

In Fig. 3 (inset) we show the perfect match between the numerical simulations of r (symbols) and the numerical solution of $r = \mathrm{Re}\{I(r,\psi)\}$ (lines) for different values of

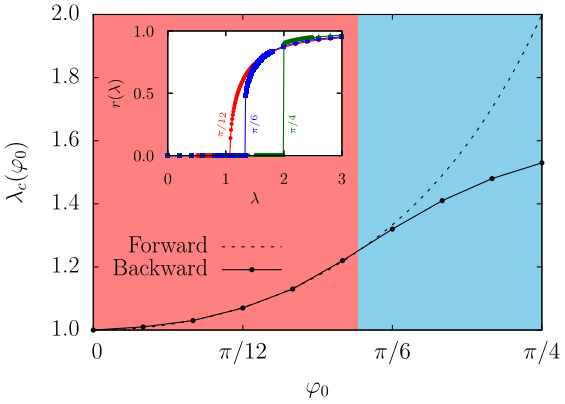

FIG. 3. Inset: Order parameter $r(\lambda)$ in a forward continuation for different values of φ_0. Points (solid lines) represent numerical simulations (theoretical predictions). Main: Threshold value λ_c as a function of φ_0. We compare it by following a forward (dashed line, λ_c) and backward (solid line, λ_u) continuations in λ of the phase transition, obtained as the theoretical prediction given by Eq. (9) and numerical simulations, respectively. The plot is colored in red (blue) for $\varphi_0 < \varphi_c$ ($\varphi_0 > \varphi_c$), signaling the theoretical separation between continuous and explosive transitions. System size $N = 10^3$, constant conviction $\rho = 1$ ($\alpha = \infty$).

φ_0 of a quadrimodal $P(\varphi)$. One can see that the nature of the transition changes from continuous, for small values of φ_0, to discontinuous, or explosive, for large values of φ_0. In Fig. 3 (main) we further check this change, by plotting the instability threshold λ_u of the upper branch of the solution, as obtained by a backward continuation simulation; see SM V [43]. As we can see in Fig. 3 (main), for $\varphi_0 < \varphi_c$ the threshold of the upper branch λ_u coincides with the threshold λ_c for the instability of the zero solution obtained by a forward continuation, indicative of a continuous transition. For $\varphi_0 > \varphi_c$, on the other hand, $\lambda_u < \lambda_c$, signaling the hysteresis typical of explosive, discontinuous transitions.

Interestingly, the theoretical predictions of the model are also recovered by starting with an initial opinion distribution extracted from empirical ANES data. If it is polarized *and* correlated (approximately bimodal $P(\varphi)$), the depolarization is continuous. For instance, Fig. 4(a) shows the topics "religion providing guidance in day-to-day living" and "business owners are allowed to refuse services to same-sex couples if they violate their religious beliefs." If instead topics are polarized but uncorrelated, represented by a quadrimodal $P(\varphi)$, we observe an explosive depolarization with hysteresis. Figure 4(b) considers topics "children of unauthorized immigrants born in the U.S. should automatically get citizenship" and "the U.S. should send troops to fight Islamic militants." These results, in full agreement with the theoretical analysis, are confirmed by other examples of polarized initial opinion distributions from the ANES dataset, detailed in SM VI [43].

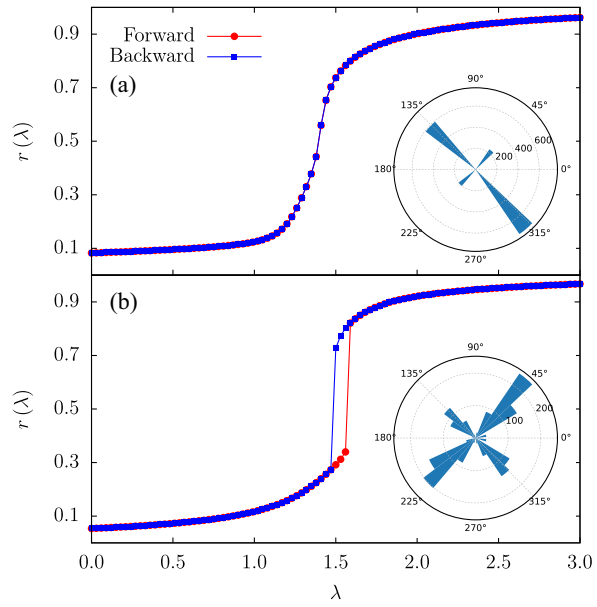

FIG. 4. Main: Order parameter $r(\lambda)$ including both forward (red) and backward (blue) continuations in λ. We consider correlated (a) and uncorrelated (b) empirical opinions from ANES data as $P(\varphi)$. Inset: Initial orientation distributions represented in polar coordinates at $\lambda = 0$. These empirical distributions are obtained neglecting all individuals with conviction lower than the median of $P(\rho)$, approaching then the case $\alpha \to \infty$.

Here we investigated how social influence can counter polarization, by proposing a simple analytically tractable mean-field opinion dynamics model. In our model, an initial polarized state undergoes a depolarization transition to a consensus state, whose nature depends on the initial correlations between opinions: the depolarization is explosive (first order) when the initial opinions are uncorrelated. Our theoretical calculations are confirmed by numerical simulations based on real opinion patterns as the initial polarization collected from the ANES dataset. The model we propose represents a first step toward understanding the evolution of polarization in interdependent topics, in a very simple and intuitive setting.

Our Letter, however, is not exempt from limitations. We considered a mean-field setting in which all individuals interact with everyone else. While this setting can be realistic for small interacting groups, interactions between agents are usually mediated by social networks: Future work should be dedicated to extending our analysis to networked substrates. Furthermore, we assumed the conviction of individuals to be constant in time, while it is reasonable that individuals change their conviction while changing orientation with respect to the two topics. Finally, the social compass model could be easily extended to n topics, mapped in terms of spherical coordinates in n dimensions, where the key assumption of the model (i.e., the stubbornness of individuals proportional to their conviction) still holds.

J. O. and R. P.-S. acknowledge financial support from the Spanish MCIN/AEI/10.13039/501100011033, under Project No. PID2019–106290GB-C21.

*Corresponding author.
michele.starnini@gmail.com
†Corresponding author.
romualdo.pastor@upc.edu

[1] S. L. Perry, Annu. Rev. Sociol. **48**, 87 (2022).
[2] J. G. Montalvo and M. Reynal-Querol, Am. Econ. Rev. **95**, 796 (2005).
[3] A. M. McCright and R. E. Dunlap, Sociol. Q. **52**, 155 (2011).
[4] J. McCoy, T. Rahman, and M. Somer, Am. Behav. Sci. **62**, 16 (2018).
[5] S. Iyengar, G. Sood, and Y. Lelkes, Publ. Opin. Q. **76**, 405 (2012).
[6] Z. Wang, M. Jusup, H. Guo, L. Shi, S. Geček, M. Anand, M. Perc, C. T. Bauch, J. Kurths, S. Boccaletti *et al.*, Proc. Natl. Acad. Sci. U.S.A. **117**, 17650 (2020).
[7] G. Michael, Skeptic **22**, 9 (2017).
[8] P. Dandekar, A. Goel, and D. T. Lee, Proc. Natl. Acad. Sci. U.S.A. **110**, 5791 (2013).
[9] F. Baumann, P. Lorenz-Spreen, I. M. Sokolov, and M. Starnini, Phys. Rev. Lett. **124**, 048301 (2020).
[10] G. Deffuant, D. Neau, F. Amblard, and G. Weisbuch, Advs. Complex Syst. **03**, 87 (2000).
[11] R. Hegselmann and U. Krause, J. Artif. Soc. Social Simul. **5**, 1 (2002).
[12] J. Lorenz, Int. J. Mod. Phys. C **18**, 1819 (2007).
[13] S. Huet, G. Deffuant, and W. Jager, Advs. Complex Syst. **11**, 529 (2008).
[14] C. Crawford, L. Brooks, and S. Sen, in *Proceedings of the 2013 International Conference on Autonomous Agents and Multi-Agent Systems (AAMAS'13)* (International Foundation for Autonomous Agents and Multiagent Systems, Richland, SC, 2013), pp. 1225–1226.
[15] A. Vinokur and E. Burnstein, J. Pers. Soc. Psychol. **36**, 872 (1978).
[16] A. Matakos, E. Terzi, and P. Tsaparas, Data Min. Knowl. Disc. **31**, 1480 (2017).
[17] C. Musco, C. Musco, and C. E. Tsourakakis, in *Proceedings of the 2018 World Wide Web Conference (WWW '18)* (International World Wide Web Conferences Steering Committee, Republic and Canton of Geneva, 2018), pp. 369–378.
[18] S. Balietti, L. Getoor, D. G. Goldstein, and D. J. Watts, Proc. Natl. Acad. Sci. U.S.A. **118**, e2112552118 (2021).
[19] W. Jager and F. Amblard, Comput. Math. Org. Theory **10**, 295 (2005).
[20] H. F. Chau, C. Y. Wong, F. K. Chow, and C.-H. F. Fung, Physica (Amsterdam) **415A**, 133 (2014).
[21] K. T. Poole, *Spatial Models of Parliamentary Voting*, Analytical Methods for Social Research (Cambridge University Press, Cambridge, England, 2005).
[22] K. Benoit and M. Laver, Eur. Union Polit. **13**, 194 (2012).

[23] J. Li and R. Xiao, J. Artif. Soc. Social Simul. **20**, 4 (2017).
[24] H. L. J. van der Maas, J. Dalege, and L. Waldorp, J. Complex Netw. **8**, cnaa010 (2020).
[25] S. Schweighofer, D. Garcia, and F. Schweitzer, Chaos **30**, 093139 (2020).
[26] T. Chen, Y. Wang, J. Yang, and G. Cong, Int. J. Environ. Res. Public Health **18**, 472 (2021).
[27] P. DiMaggio, J. Evans, and B. Bryson, Am. J. Sociol. **102**, 690 (1996).
[28] D. Baldassarri and A. Gelman, Am. J. Soc. **114**, 408 (2008).
[29] A. Freire, Party Polit. **14**, 189 (2008).
[30] F. Falck, J. Marstaller, N. Stoehr, S. Maucher, J. Ren, A. Thalhammer, A. Rettinger, and R. Studer, Policy Internet **12**, 367 (2020).
[31] A. Adamczyk, Eur. Sociol. Rev. **38**, 816 (2022).
[32] D. DellaPosta, Y. Shi, and M. Macy, Am. J. Sociol. **120**, 1473 (2015).
[33] M. F. Laguna, G. Abramson, and D. H. Zanette, Physica (Amsterdam) **329A**, 459 (2003).
[34] S. Fortunato, V. Latora, A. Pluchino, and A. Rapisarda, Int. J. Mod. Phys. C **16**, 1535 (2005).
[35] S. R. Etesami, T. Baar, A. Nedi, and B. Touri, in *Proceedings of the 2013 American Control Conference* (IEEE, Washington, DC, 2013), pp. 1255–1260, ISSN: 2378-5861.
[36] P. E. Converse, Crit. Rev. **18**, 1 (2006).
[37] F. Baumann, P. Lorenz-Spreen, I. M. Sokolov, and M. Starnini, Phys. Rev. X **11**, 011012 (2021).
[38] R. P. Abelson, Am. Psychol. **43**, 267 (1988).
[39] A. G. Miller, J. W. McHoskey, C. M. Bane, and T. G. Dowd, J. Pers. Soc. Psychol. **64**, 561 (1993).
[40] E. M. Pomerantz, S. Chaiken, and R. S. Tordesillas, J. Pers. Soc. Psychol. **69**, 408 (1995).
[41] http://www.politicalcompass.org.
[42] http://www.electionstudies.org.
[43] See Supplemental Material at http://link.aps.org/supplemental/10.1103/PhysRevLett.130.207401 for details regarding the empirical data set considered, the analytical solution of the model, and numerical simulation.
[44] N. E. Friedkin and E. C. Johnsen, J. Math. Sociol. **15**, 193 (1990).
[45] A. Pluchino, V. Latora, and A. Rapisarda, Int. J. Mod. Phys. C **16**, 515 (2005).
[46] C. Castellano, S. Fortunato, and V. Loreto, Rev. Mod. Phys. **81**, 591 (2009).
[47] Y. Kuramoto, in *Proceedings of the International Symposium on Mathematical Problems in Theoretical Physics*, edited by H. Araki (Springer, New York, 1975), pp. 420–422.
[48] J. A. Acebrn, L. L. Bonilla, C. J. P. Vicente, F. Ritort, and R. Spigler, Rev. Mod. Phys. **77**, 137 (2005).
[49] M. Abramowitz and I. A. Stegun, *Handbook of Mathematical Functions* (Dover, New York, 1972).